

# NONDESTRUCTIVE EVALUATION OF FATIGUE DAMAGE USING MAGNETIC MEASUREMENT TECHNIQUES

C. C. H. Lo<sup>2</sup>, F. Tang<sup>2</sup>, Y. Shi<sup>1</sup>, D. C. Jiles<sup>1,2</sup> and S. B. Biner<sup>1,2</sup>

<sup>1</sup>Center for NDE  
<sup>2</sup>Ames Laboratory  
Iowa State University  
Ames, Iowa 50011

## INTRODUCTION

Fatigue is responsible for most of the mechanically-induced service failures of structural components encountered in industry. Therefore there is a pressing need for the development of nondestructive evaluation (NDE) methods to detect the development of fatigue damage, to monitor its progress and to predict impending failure of components as they come close to the end of their fatigue lives. Magnetic measurements offer promising techniques for these purposes, since the magnetic properties of ferromagnetic materials are sensitive to the microstructural changes caused by fatigue damage [1].

Previous studies have been made on the variations in magnetic properties with stress cycling [2-5]. Recently significant progress has been made to develop magnetic measurement techniques to monitor fatigue damage [6-9]. It has been shown that fatigue lifetime is related to the pre-fatigue magnetic properties [8]. Magnetic hysteresis properties, such as coercivity and remanence, were found to change drastically in the final stages of fatigue [8,9]. These results suggest that it is possible to predict the onset of catastrophic failure by measuring these magnetic properties. Nevertheless very little change in these parameters was observed in the intermediate stage of fatigue when the dislocation structure inside the materials became stabilized [8,9]. This raises the need of further research in order to advance our understanding of the variations in microstructure-sensitive magnetic properties with fatigue damage.

The present paper reports a systematic study of the changes in magnetic properties and microstructure caused by fatigue. The ultimate objective of this investigation is to find out the magnetic properties whose variations with fatigue cycling can be used as a measure of the accumulation of fatigue damage, and to develop the measurement techniques of these magnetic properties as viable methods for monitoring the remaining fatigue lifetime of structural components.

## EXPERIMENTAL DETAILS

Two 0.2wt% C Fe-C alloy bars, designated as S1 and S2, were austenitized at 905°C and 1050°C respectively for 2 hours and then furnace cooled at a rate of 2°C/min. The heat-treated samples were found to have a ferrite/pearlite structure with a pearlite content of about 21%. The measured ferrite grain sizes of the samples are shown in Table I. The samples were machined to an “hour glass” shape with a minimum diameter of 6 mm at the sample centre, and were then carefully ground and electro-polished to obtain a smooth surface finish.

Strain-controlled fatigue tests were carried out using a computer-controlled servo-hydraulic mechanical testing system. The baseline magnetic properties of the samples were measured before the samples were cycled. During a fatigue test the sample was cyclic-strained at 2 Hz with a strain amplitude of 0.2%. The test was halted at pre-determined intervals under the zero strain condition. In-situ measurements of magnetic hysteresis loops were made using the Magnescope, an instrument developed at Iowa State University. Bulk magnetic parameters such as coercivity  $H_c$ , remanence  $B_r$  and initial permeability  $\mu_i$  were measured. The average measurement errors of these parameters were found to be about 1%. Plastic replicas were prepared and examined using scanning electron microscope (SEM) in order to study the microstructural changes of the sample surface during fatigue.

## RESULTS AND DISCUSSION

The baseline magnetic properties of the samples are shown in Table I. It was found that S1 had larger baseline coercivity  $H_{c0}$  and remanence  $B_{r0}$  than S2. It is due to the fact that S1 had smaller grain size which gave rise to stronger pinning of magnetic domain walls at the grain boundaries than in S2. The variations in  $H_c$  and  $B_r$  of these samples with expended fatigue life are shown in Figures 1 and 2 respectively. The fatigue life of the samples can be divided into three stages according to the variations in the mechanical and magnetic properties. In stage I (about the first 10% of fatigue life) significant increase in  $H_c$  and  $B_r$  was observed. This is probably caused by fatigue hardening during which the dislocation density inside the samples increased rapidly with cyclic deformation. The increase in dislocation interactions with magnetic domain walls resulted in stronger impedance to domain wall movement, causing  $H_c$  to increase. It was also found that  $H_c$  and  $B_r$  of S1 increased to higher levels (i.e. larger  $H_{cs}$  and  $B_{rs}$ ) at the end of stage I than those of S2. In stage II (10% to about 86%)  $B_r$  remained unchanged while  $H_c$  tended to increase. The loads required to maintain the pre-determined strain level were found to stabilize. In this stage the existing dislocations moved to and accumulated at the sample surface, resulting in the formation of slip lines. Therefore the increase in  $H_c$  is probably related to the increase in dislocation density in the surface layer. In stage III  $H_c$  and  $B_r$  decreased dramatically until the samples were fractured. In this stage the formation and propagation of macroscopic fatigue cracks produced strong demagnetizing effect and flux leakage at the crack, making it more difficult to magnetize the sample to saturation. As a result  $H_c$  and  $B_r$  decreased.

Table I. The ferrite grain sizes, fatigue lifetimes and baseline magnetic properties of samples S1 and S2.

| Sample | ferrite grain size<br>( $\mu\text{m}$ ) | Fatigue lifetime<br>(number of fatigue cycle) | $H_{c0}$<br>(Oe) | $B_{r0}$<br>(G) | $\mu_{i0}$ |
|--------|---|---|------------------|-----------------|------------|
| S1     | 24                                      | 29800   | 2.35             | 1806            | 422        |
| S2     | 59                                      | 23800   | 2.11             | 1487            | 406        |

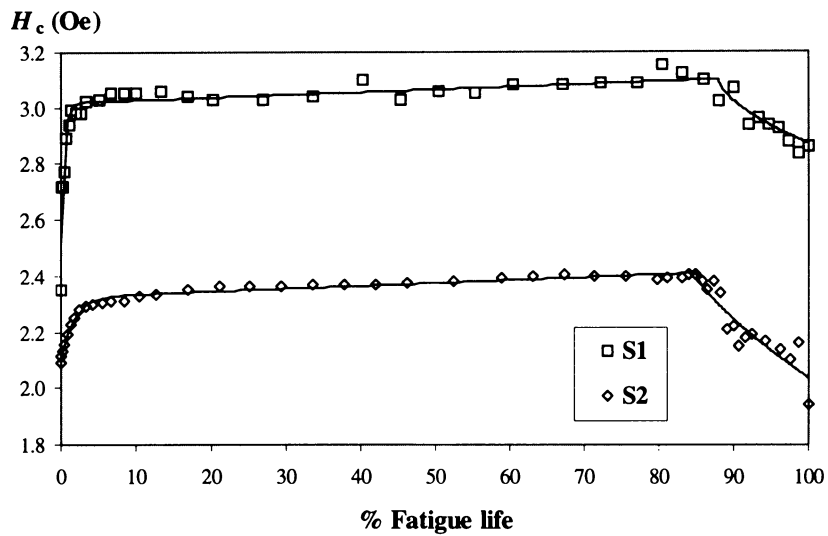


Figure 1. Variation in coercivity  $H_c$  with % fatigue life  $n$  for samples S1 and S2. The fitting of Equation (1) to the experimental data are shown as solid lines.

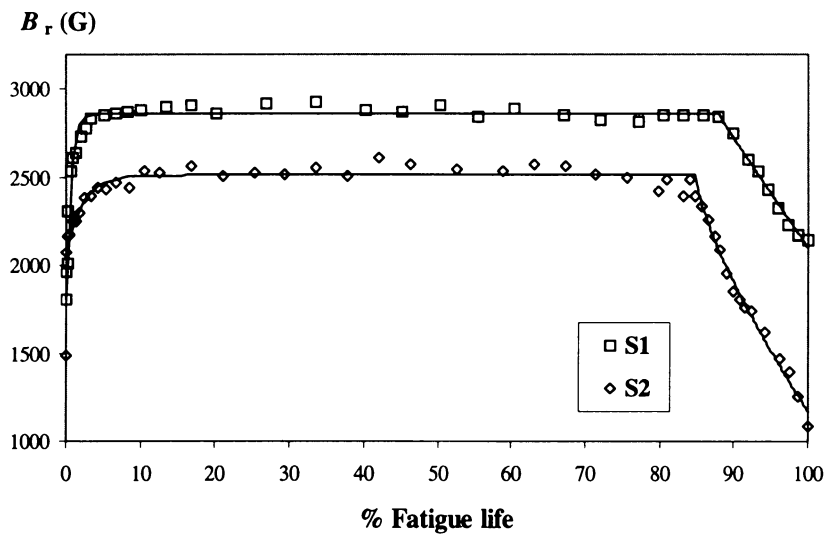


Figure 2. Variation in remanence  $B_r$  with % fatigue life  $n$  for samples S1 and S2. The fitting of Equation (2) to the experimental data are shown as solid lines.

In a previous study model equations have been proposed to describe the variations in mechanical modulus and magnetic remanence with fatigue cycle [10]. These equations were developed by assuming that the bulk dislocation density and hence the magnetic remanence decrease exponentially with fatigue during the fatigue softening stage, remain constant during the stable fatigue stage and decrease in the final stages of fatigue when the fatigue cracks grow. Since  $H_c$  is also related to dislocation density [11], it is expected that the model equations can be applied to describe the changes in  $H_c$  during fatigue. In the present study it was proposed that the variations in  $H_c$  and  $B_r$  with  $n$  can be described by:

$$H_c = \kappa \left[ H_{cs} - (H_{cs} - H_{c0}) e^{-\frac{n}{R_H}} + \alpha_H n \right] + (1 - \kappa) \left[ H_{n0} + d_H (n - n_0)^{c_H} \right] \quad \text{and (1)}$$

$$B_r = \kappa \left[ B_{rs} - (B_{rs} - B_{r0}) e^{-\frac{n}{R_B}} \right] + (1 - \kappa) \left[ B_{n0} + d_B (n - n_0)^{c_B} \right], \quad (2)$$

where  $\kappa = 1$  for  $n < n_0$ , and  $\kappa = 0$  for  $n \geq n_0$ .  $n_0$  denotes the onset of stage III when the magnetic properties started to decrease dramatically due to the formation and propagation of macroscopic fatigue cracks.

Equations (1) and (2) are similar to the model equation proposed in the previous study except for a few modifications. The first two terms of the above equations describe the exponential increase in  $H_c$  and  $B_r$  from the initial values to the levels  $H_{cs}$  and  $B_{rs}$  during the fatigue hardening stage. A linear term  $\alpha_H n$  was added to Equation (1) to describe the increase in  $H_c$  during stage II which is probably related to the increase in dislocation density in the surface layer, since the bulk dislocation structure should be stable in this stage. The parameters obtained by fitting Equations (1) and (2) to the experimental results are listed in Table II. The viability of coercivity measurement as a method for monitoring remaining fatigue lifetime is determined by the sensitivity of  $H_c$  to  $n$  in stage II. This can be estimated by dividing  $\alpha_H$  by  $H_{cs}$  (refer to Table II). The results show that  $H_c$  increases by about 0.03% and 0.04% per percentage increase in fatigue life for S1 and S2 respectively. Taking the measurement error of  $H_c$  into account, the uncertainty of estimating the

Table II. Parameters obtained by fitting Equations (1), (2) and (3) to the experimental data of  $H_c$ ,  $B_r$  and  $\mu_i$  as functions of  $n$  for samples S1 and S2.

| Equation (1) |               |         |                      |           |              |               |         |
|--------------|---------------|---------|----------------------|-----------|--------------|---------------|---------|
| Sample       | $H_{cs}$ (Oe) | $R_H$   | $\alpha_H$           | $n_0$ (%) | $d_H$        | $H_{n0}$ (Oe) | $c_H$   |
| S1           | 3.02          | -0.42   | $0.9 \times 10^{-3}$ | 87.9      | -0.05        | 3.08          | 0.61    |
| S2           | 2.32          | -1.76   | $1.0 \times 10^{-3}$ | 84.8      | -0.05        | 2.41          | 0.75    |
| Equation (2) |               |         |                      |           |              |               |         |
| Sample       | $B_{rs}$ (G)  | $R_B$   | $n_0$ (%)            | $d_B$     | $B_{n0}$ (G) | $c_B$         |         |
| S1           | 2862          | -0.06   | 87.9                 | -69.0     | 2862         | 0.96          |         |
| S2           | 2512          | -2.24   | 84.8                 | -182.3    | 2512         | 0.73          |         |
| Equation (3) |               |         |                      |           |              |               |         |
| Sample       | $\mu_{is}$    | $R_\mu$ | $\alpha_\mu$         | $n_0$ (%) | $d_\mu$      | $\mu_{n0}$    | $c_\mu$ |
| S1           | 491           | -1.35   | -0.48                | 87.9      | -0.08        | 448           | 2.78    |
| S2           | 638           | -0.48   | -0.53                | 84.8      | -22.50       | 591           | 0.79    |

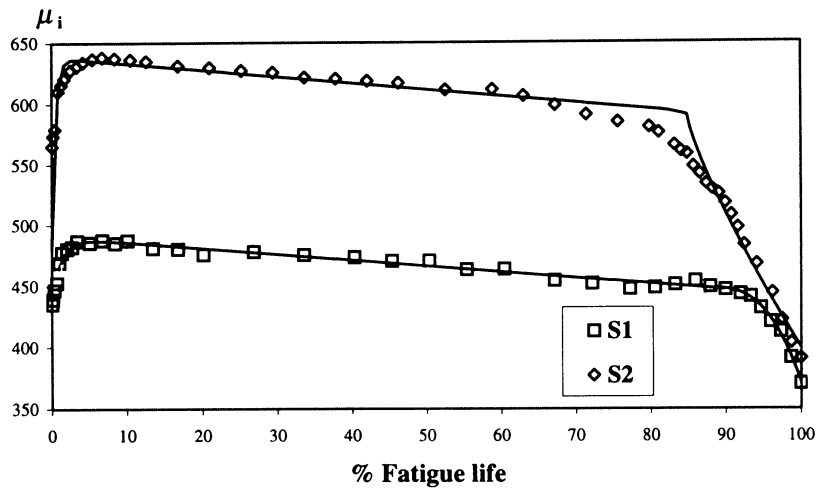


Figure 3. Variations in initial permeability  $\mu_i$  with % fatigue life  $n$  for samples S1 and S2. The fitting of Equation (3) to the experimental data are shown as solid lines.

remaining percentage fatigue lifetime by coercivity measurements was found to be about 25%. This result shows that coercivity measurements may not be suitable as an NDE method for monitoring remaining fatigue lifetime because of the low sensitivity of  $H_c$  to the accumulation of fatigue damage during the stable fatigue stage.

Figure 3 shows the dependence of initial permeability  $\mu_i$  on  $n$  for samples S1 and S2. Similar to  $H_c$  and  $B_r$ ,  $\mu_i$  increased dramatically in stage I and decreased significantly in stage III. It is worth noticing that  $\mu_i$  decreased with increasing  $n$  in stage II. This is probably caused by the increase in dislocation density in the surface layer which limits the extent of reversible domain wall movement. Similar to  $H_c$ ,  $\mu_i$  is also dependent on the dislocation density. This suggests that the variation in  $\mu_i$  with  $n$  can be described by:

$$\mu_i = \kappa \left[ \mu_{is} - (\mu_{is} - \mu_{i0}) e^{-\frac{n}{R_\mu}} + \alpha_\mu n \right] + (1 - \kappa) \left[ \mu_{n0} + d_\mu (n - n_0)^{c_\mu} \right] \quad (3)$$

which is similar to Equation (1). The parameters obtained by fitting Equation (3) to the experimental results are shown in Table II. It was found that in stage II  $\mu_i$  decreased by about 8% and 13% for specimens S1 and S2 respectively. The rates at which  $\mu_i$  decreased with  $n$  in stage II (estimated by dividing  $\alpha_\mu$  by  $\mu_{is}$ ) were found to be 0.10 and 0.09% per percentage increase in fatigue life for S1 and S2 respectively. This shows that  $\mu_i$  is more sensitive than  $H_c$  and  $B_r$  to the accumulation of fatigue damage in the stable fatigue stage. Taking the measurement error of  $\mu_i$  into account, the uncertainty of the estimation of remaining fatigue lifetime by measuring  $\mu_i$  is about 10%. The present results therefore suggest that the measurement of initial permeability can be used as a promising method for monitoring remaining fatigue lifetime. Further research is in progress to improve the sensitivity and accuracy of the initial permeability measurement in order to develop it as a viable NDE technique to evaluate fatigue damage in steel components.

Figure 4 shows the SEM micrographs of the replicas taken from the samples at various stages of fatigue. Formation of slip bands were readily observed in both samples at

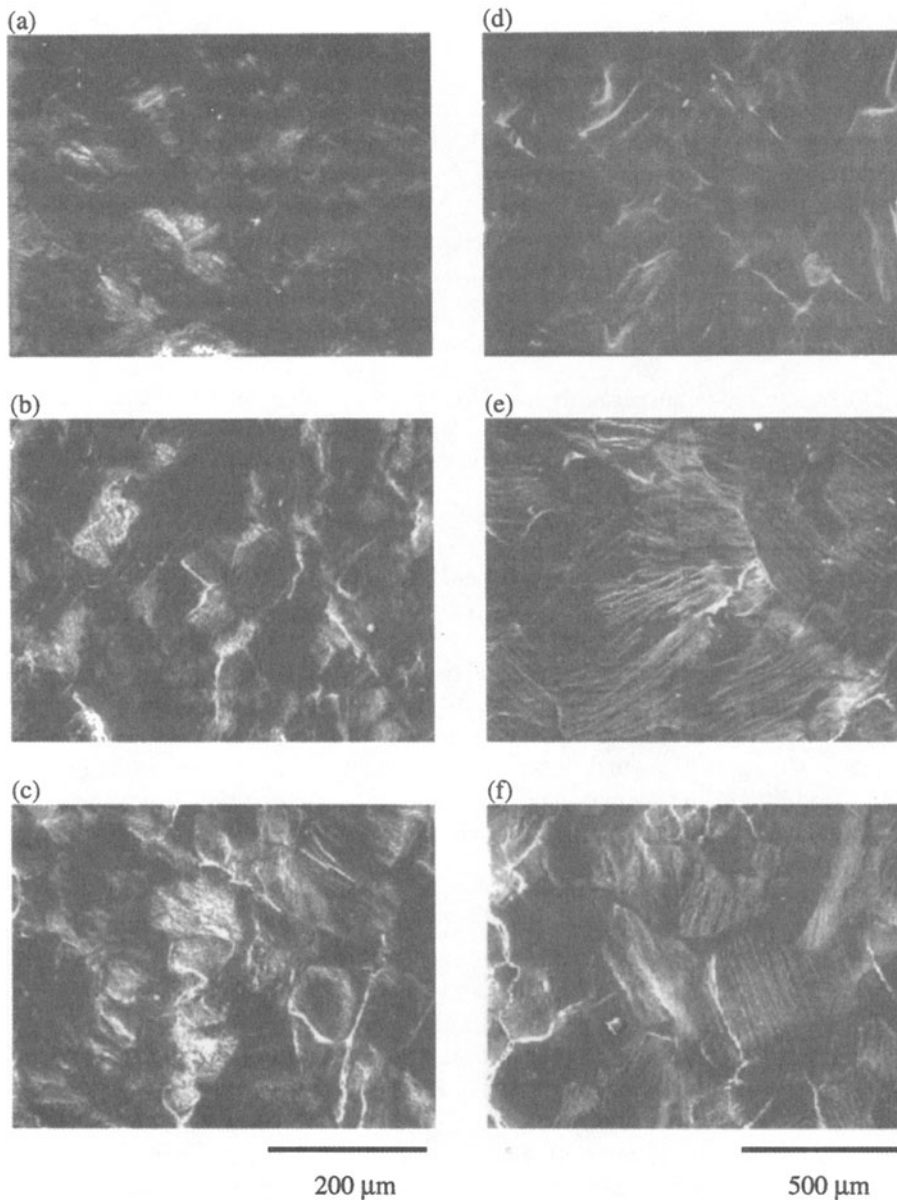


Figure 4. SEM micrographs of the surface replicas taken at (a) 16%, (b) 49% and (c) 88% of fatigue life from sample S1 and at (d) 14%, (e) 43% and (f) 86% of fatigue life from sample S2.

about 15% fatigue life (Figure 4a and 4d). The amount of slip bands was found to increase throughout stage II. Formation of microcracks was also observed in this stage (Figure 4b and 4e). As these formed the mean dislocation separation became smaller, giving rise to stronger impedance to domain wall motion. As a result  $H_c$  increased and  $\mu_i$  decreased. Upon further cyclic deformation propagation and linking of microcracks took place (Figure 4c and 4f). These processes led to the formation of macrocracks which then grew and eventually caused the samples to fail.

The different responses of the magnetic properties of samples S1 and S2 to fatigue cycling can be interpreted in terms of the fatigue-induced changes in microstructure. In stage I, the dislocations created inside the samples piled up at the grain boundaries, forming a cellular structure which became stabilized at the end of stage I. The dislocation cell walls became the dominant pinning sites of domain walls, and hence the magnetic properties were dependent on the dislocation cell size which was determined by the grain size of the sample. A finer grain structure gives rise to smaller dislocation cell size and hence stronger domain wall pinning. This could be the reason why at the end of stage I  $H_c$  and  $B_r$  increased to higher levels while  $\mu_i$  decreased to a lower level for sample S1 than for S2. In stage II the changes in  $\mu_i$  could be related to the accumulation of fatigue damage in the surface layer. Therefore it is expected that the sample with more severe fatigue damage in its surface layer should show a larger reduction in  $\mu_i$  in stage II. This speculation is supported by the present results which show that  $\mu_i$  of S2 decreased by a larger percentage (13%) than that of S1 (8%) over stage II.

## CONCLUSIONS

The results of this study have demonstrated that magnetic measurement techniques are viable NDE methods for evaluating fatigue damage in steel components. A significant decrease in the magnetic properties such as coercivity, remanence and initial permeability observed in the final stages of fatigue indicates that the measurements of these parameters are promising methods for predicting impending failure. In the stable fatigue stage it was found that coercivity increased slightly while initial permeability decreased. These changes can be attributed to increasing impedance to domain wall motion due to the accumulation of fatigue damage in the surface layer. In this stage it was also found that initial permeability was more sensitive to fatigue cycling than coercivity and remanence. The present results therefore indicate that the measurement of initial permeability can be developed as a viable NDE technique to estimate the remaining fatigue lifetime and hence to monitor fatigue damage throughout the whole fatigue life of steel components.

## ACKNOWLEDGEMENTS

This work was supported by National Science Foundation, Division of Civil and Mechanical Structures under the grant number CMS-9532056.

## REFERENCES

1. D. C. Jiles, NDT International, **21**, 311 (1988).
2. M. B. Shah, and M. S. C. Bose, phys. stat. sol.(a), **86**, 275 (1984).
3. M. S. C. Bose, NDT International, **19**, 83 (1986).
4. C. H. A. Sanford-Francis, Brit J NDT, **23**, 241 (1981)
5. C. H. A. Sanford-Francis, Brit J NDT, **29**, 83 (1987)
6. M. K. Devine, D. C. Jiles, and S. Hariharan, J. Magn. Magn. Mater., **104**, 377 (1992).

7. Z. J. Chen, D. C. Jiles, and J. Kameda, *J. Appl. Phys.*, **75(10)**, 6975 (1994).
8. Y. Bi, M. R. Govindaraju, and D. C. Jiles, *IEEE Trans. Magn.*, **32**, 3928 (1997).
9. M. R. Govindaraju, A. Strom, D. C. Jiles and S. B. Biner, in *Review of Progress of QNDE*, Vol. 12, eds. D. O. Thompson and D. E. Chimenti (Plenum, New York, 1993), p. 1839.
10. Y. Bi, "The dynamic variations of magnetic properties of steel due to cyclic loading", MSc Thesis, Iowa State University, 1997.
11. D. C. Jiles, *Introduction to Magnetism and Magnetic Materials*, 2nd ed. (Chapman and Hall, London, 1998), Chap. 8.